

Linear theory of the free-electron laser with a two-frequency undulator

Zhi-Min Dai, Xiao-Feng Zhao, and Fu-Jia Yang

Institute of Nuclear Research, Academia Sinica, P.O. Box 800-204, Shanghai 201800, China

(Received 4 January 1994)

In this paper, a linear analysis of the free-electron laser with a two-frequency undulator in the high-gain regime is presented. The two-frequency undulator induces a beating wave in the electron's longitudinal motion, which results in many resonant points in phase space. As the electron's beating wave motion causes emission into many unstable modes, it reduces the maximum growth rate for the most unstable mode. Our analysis shows that, under proper conditions, the ponderomotive phase velocity of the most unstable mode may be reduced by the complex interferences between different resonant points, leading to an efficiency enhancement. Moreover, optical guiding in this device is also studied. It is found that the electron's beating wave motion may reduce the refractive guiding and enhance the power coupling coefficient of the most unstable mode.

PACS number(s): 41.60.Cr, 52.40.Mj, 52.75.Ms

I. INTRODUCTION

In a free-electron laser (FEL), a relativistic beam of electrons passes through a periodic transverse magnetic field, the undulator or wiggler, to produce coherent radiation [1–3]. One of the main advantages of the FEL is that it may provide a source of coherent radiation from the far infrared to the vacuum ultraviolet region. To reach the high-power Compton regime, however, FELs are characterized by strong spectral broadenings [4,5]. Although some technical solutions have been implemented [5], they may lead to severe drawbacks such as threshold damage or nontunability. Recently, a FEL amplifier in the configuration with a two-frequency undulator (TFU) is suggested [6,7] in order to obtain a better extraction efficiency and a narrower radiation spectrum compared with those provided by an ordinary (one-frequency) undulator.

The TFU is taped by introducing a second frequency in the undulator magnetic field to alter the dynamics of the relativistic electrons. The period of the second frequency ($\lambda_{w2}=2\pi/k_{w2}$) is assumed to be closed to that of the first frequency ($\lambda_{w1}=2\pi/k_{w1}$). As a relativistic electron passes through the TFU, it executes a beating wave ($\lambda_b=2\pi/k_b$) in its longitudinal motion, where $k_b=k_{w1}-k_{w2}$. The electron's longitudinal beating wave motion (EBW) may modify the FEL dynamics in both a linear regime and a nonlinear regime.

The effects of the EBW on the spontaneous emission and on the stimulated emission in the low-gain regime and saturation regime have been studied in Refs. [6,7]. In this paper, we present a linear theory of the FEL amplifier with a TFU. Our main purpose is to show the effects of the EBW on the stimulated emission in the high-gain regime and on optical guiding in this device. This paper is organized as follows. First, in Sec. II a set of one-dimensional nonlinear equations is developed to describe the evolution of the radiation field in this device. In Sec. III these nonlinear equations for the TFU FEL are analyzed in the weak-field high-gain regime to evalu-

ate the growth rate and the extraction efficiency. Moreover, optical guiding in the TFU FEL is studied in Sec. IV. Finally, a summary is given in Sec. V.

II. BASIC DYNAMICS OF THE FREE-ELECTRON LASER WITH A TWO-FREQUENCY UNDULATOR

The TFU FEL consists of a relativistic beam of electrons propagating parallel to a transverse magnetic field with two periods. The magnetic field of the TFU may be taken to be

$$\mathbf{B}_w = [B_{w1}\sin(k_{w1}z) + B_{w2}\sin(k_{w2}z)]\hat{y}, \quad (2.1)$$

where B_{w1} and B_{w2} are the amplitudes of the magnetic field with respect to the first period and second period, respectively, with $B_{w2} \ll B_{w1}$. Since the second period induces a slow modulation of the first period, a TFU may be designed by varying the magnetic amplitude of an ordinary undulator.

As a relativistic electron travels through the TFU, it executes transverse oscillations, which may be expressed by

$$\mathbf{v}_\perp = -\frac{c}{\gamma} [K_1 \cos(k_{w1}z) + K_2 \cos(k_{w2}z)]\hat{x}, \quad (2.2)$$

where $K_l = eB_{wl}\lambda_{wl}/2\pi m_e c^2$ is the undulator strength parameter for $l=1,2$, γ is the Lorentz factor of the relativistic electron, c is the period of light, and m_e and e are the rest mass and charge of the electron, respectively. The electron's transverse motion directly couples to its longitudinal motion and causes some fluctuations ($2k_{w1}, 2k_{w2}, k_{w1}+k_{w2}, k_b$ modulations) in its longitudinal motion. Compared to the motion in an ordinary undulator [8–11], the electron's motion in the TFU has two new features. The first is that the electron's transverse oscillations in a TFU are the sum of two terms corresponding to the two undulator periods, respectively. Because $B_{w2} \ll B_{w1}$, this is not an essential feature, and then the energy extraction from the relativistic electron beam

corresponding to the second term of Eq. (2.2) may be neglected. The second feature is the beating wave (k_b modulation) in the electron's longitudinal motion. This is the basic characteristic of the TFU FEL, which may modify the FEL dynamics in both the linear regime and the nonlinear regime. Therefore, we will focus our attention on the effects of the EBW on the FEL dynamics. In addition, the electron's longitudinal fast oscillations ($2k_{w1}, 2k_{w2}, k_{w1} + k_{w2}$ modulations) may cause emission into higher harmonics and reduce the gain of the fundamental, which is important in the harmonic generation in the FEL [12,13]. For simplicity, we neglect the effects of longitudinal fast oscillations on the FEL dynamics. As a result, electron's longitudinal trajectories may be written as $z = \bar{z} + \Delta z$, where $\bar{z} = \bar{v}_z t$ is the longitudinal location assuming that the electron has uniform longitudinal velocity $\bar{v}_z = [1 - (1 + a_w^2)/2\gamma^2]c$, with $a_w^2 = (K_1^2 + K_2^2)/2$, and the EBW is given by

$$\Delta z = -K_1 K_2 \sin(k_b \bar{z}) / 2\gamma^2 k_b. \quad (2.3)$$

Obviously, the EBW will yield an oscillation of the electron's phase, which is

$$k \Delta z \approx -\sigma \sin(k_b \bar{z}), \quad (2.4)$$

where $\sigma = K_1 K_2 k_{w1} / k_b$ and k is the wave number of optical field. Since bunching on the optical wavelength scale is the key element of the stimulated emission process, the EBW becomes important when its amplitude is comparable to the optical wavelength $\lambda = 2\pi/k$. Thus the FEL dynamics may be deeply modified by the EBW when $\sigma \approx 1$.

To study the resonant interaction between the relativistic electrons and the optical field through the TFU, we take the vector potential of the optical field to be

$$\mathbf{A} = \frac{E_s}{k} \sin(kz - \omega t + \varphi) \hat{\mathbf{x}}, \quad (2.5)$$

where E_s and φ are the slowly varying optical amplitude and phase, respectively, and $\omega = kc$ is the optical frequency. The evolution of the optical field in the TFU is determined by the coupled Maxwell and Lorentz equations. Following the classical technique [14], the coupled Maxwell and Lorentz equations can be simplified to reduced nonlinear equations. In the limit of $B_{w2} \ll B_{w1}$, one obtains

$$\frac{d^2}{d\tau^2} \xi_s = [a_s \exp(i\xi_s) + \text{c.c.}] + \kappa^2 \sigma \sin(\kappa\tau), \quad (2.6)$$

$$\frac{d}{d\tau} a_s = -\langle \exp(-i\xi_s) \rangle, \quad (2.7)$$

where $\xi_s = (k + k_{w1})\bar{z} - \omega t$, $\tau = \bar{z}/L_G$, $\kappa = k_b L_G$, $a_s = E_s \exp(i\varphi) / \sqrt{4\pi m_e c^2 \gamma n_e \rho}$ is the dimensionless optical wave amplitude, and $L_G = \lambda_{w1} / 4\pi\rho$ is the gain length, with $\rho = \gamma^{-1} (a_w w_p / 4k_w c)^{2/3}$ and $\omega_p = \sqrt{4\pi n_e e^2 / m_e}$ (n_e is the relativistic electron density). The combined equations (2.6) and (2.7) are valid in weak or strong optical fields, for large or small gain, and for an arbitrary electron distribution. Compared to the equations for the ordinary undulator FEL [8–11], a new feature appears in

these equations, which is the driving term of the pendulum equation (2.6). When $\sigma \approx 1$, the driving term will alter the nature of both the linear regime and the nonlinear regime.

III. LINEAR ANALYSIS OF THE FREE-ELECTRON LASER WITH A TWO-FREQUENCY UNDULATOR

In the preceding section, we presented a general description of the basic dynamics of the FEL amplifier with a TFU. We now proceed to analyze the basic nonlinear equations (2.6) and (2.7) in the weak-field high-gain regime. In this case, these nonlinear equations may be linearized and the reference to the individual electron phase can be explicitly removed. Expanding these equations and keeping to the first order of the optical amplitude a_s , one obtains

$$\frac{d}{d\tau} a_s = i \int_0^\tau d\tau' \int_0^{\tau'} d\tau'' \exp\{i[\nu_0(\tau - \tau') + \sigma \sin(\kappa\tau'') - \sigma \sin(\kappa\tau)]\} a_s(\tau''), \quad (3.1)$$

where $\nu_0 = [(k + k_{w1}) - \omega / \bar{v}_z] L_G$ is the initial energy detuning. With the help of the integer-order Bessel function, Eq. (3.1) may be rewritten as

$$\frac{d}{d\tau} a_s = i \sum_{m,n=-\infty}^{\infty} J_m(\sigma) J_n(\sigma) \times \int_0^\tau d\tau' \int_0^{\tau'} d\tau'' \exp[-i(\nu_m \tau - \nu_n \tau'')] \times a_s(\tau''), \quad (3.2)$$

where $\nu_n = \nu_0 - n\kappa$, with $n = 0, \pm 1, \pm 2, \dots$, and J_n is the Bessel function of the first kind and n th order. Obviously, Eq. (3.2) presents many resonant points ($\nu_n \approx 0$) in phase space, which is a result of the linearized equation of the forced pendulum equation (2.6) being a driven harmonic oscillator equation. This is different from the linearized equation for the conventional FEL, which presents only one resonant point in phase space.

In the high-gain regime, the coherent radiation field may get enough energy to grow exponentially. Then one may assume that (3.2) has a solution of the form $a_s = a_0 \exp(\int_0^\tau \beta d\tau)$ and obtain

$$\alpha = i \sum_{n=-\infty}^{\infty} S_n (\alpha + i\nu_n)^{-2}, \quad (3.3)$$

where α is defined as $\alpha = \int_0^{L_w} d\tau \beta(\tau) / L_w$ and the coupling factor S_n is given by

$$S_n = i \sum_{m=-\infty}^{\infty} J_{m+n}(\sigma) J_n(\sigma) \frac{1}{mk_b L_w} [1 - \exp(imk_b L_w)]. \quad (3.4)$$

Equation (3.3) is a general dispersion relation of the high-gain TFU FEL, which clearly presents the effects of the EBW on the FEL dynamics in the weak-field high-gain regime. In the limit of $\sigma \ll 1$, $S_n \approx 1$ for $n = 0$ and

$S_n \approx 0$ for $n \neq 0$. Then Eq. (3.3) will be reduced to the well-known cubic equation for the standard FEL or traveling tube [10]. The validity of the dispersion relation requires

$$\frac{d}{d\tau} \alpha \ll (\alpha + i\nu_n)^{-2}. \quad (3.5)$$

The condition Eq. (3.5) is generally lenient for $k_b L_w \geq 2\pi$, but becomes progressively restrictive as $k_b L_w$ decreases. Clearly, the condition $k_b L_w \geq 2\pi$ may be satisfied easily and then Eq. (3.3) is valid enough to describe the TFU FEL in the weak-field high-gain regime.

For simplicity, we assume that $k_b L_w \gg 2\pi$ in the following discussion. In this case, $S_n = J_n^2(\sigma)$, and Eq. (3.3) presents one stable mode with $\text{Re}(\alpha) = 0$ and many unstable modes, either increasing modes with $\text{Re}(\alpha) > 0$ or decreasing modes with $\text{Re}(\alpha) < 0$. Since our interest is in the energy extraction from the relativistic electron beam, we restrict our attention to the increasing mode. Here it is worth examining the characteristics of Eq. (3.3) in the limit of $\nu_0 \rightarrow -\infty$. As $\nu_0 \rightarrow -\infty$, Eq. (3.3) is reduced to

$$\nu_0 = -i \sum_{n=-\infty}^{\infty} S_n (\alpha + i\nu_n)^{-2}, \quad (3.6)$$

in which many increasing and decreasing modes exist, but there is only one increasing mode whose imaginary part approaches $-\nu_n$ for $\nu_0 \rightarrow -\infty$. Therefore, we may label the increasing mode whose imaginary part approaches $-\nu_n$ for $\nu_0 \rightarrow -\infty$ as the n th unstable mode for the high-gain TFU FEL.

There are three regimes of the high-gain TFU FEL, depending on the value of κ . For $\kappa \ll 1$, the maximum growth rate of the zeroth mode ($n=0$) is much larger than the growth rate of the others modes [Fig. 1(a)], and the spectrum of the zeroth mode is similar to the usual shape for the FEL with an ordinary undulator [8–11]. When $\kappa \gg 1$, coupling is not possible between remote frequencies, and then the general dispersion relation may be reduced to

$$\alpha = iS_n (\alpha + i\nu_n)^{-2} \quad (3.7)$$

for the n th unstable mode. The spectrum of each unstable mode is similar to the well-known peak with a usual shape [Fig. 1(c)], and the radiation frequency is peaked at

$$\omega_n = [2\gamma^2 / (1 + a_w^2)] (k_{w1} - nk_b) c. \quad (3.8)$$

As $\kappa \approx 1$, complex interferences occur between the different resonant points. The spectrum of each mode is deeply modified by the complex interferences [Fig. 1(b)]. From this one may conjecture that a TFU basically modifies the high-gain FEL dynamics when the parameter κ is comparable to unity.

The eigenvalue α of the general dispersion equation (3.3) greatly depends on the TFU parameters κ and σ . Figure 2 provides an illustration in which the growth rate $\text{Re}(\alpha)$ and the phase shift rate $\text{Im}(\alpha + i\nu_0)$ of the most unstable mode at resonance are shown. Figure 2(a) shows that the growth rate of the most unstable mode decreases with σ . This is due to the EBW, which causes emission into many unstable modes and reduces the growth rate of

the most unstable mode. From Fig. 2(b), it can be seen that there exists discontinuity on the phase shift rate surface of the most unstable mode. This results from the competition between the zeroth mode ($n=0$) and the first mode ($n=1$). For small σ and κ , the growth rate of the zeroth mode is much larger than the growth rates of the other modes ($n \neq 0$), and then the zeroth mode dom-

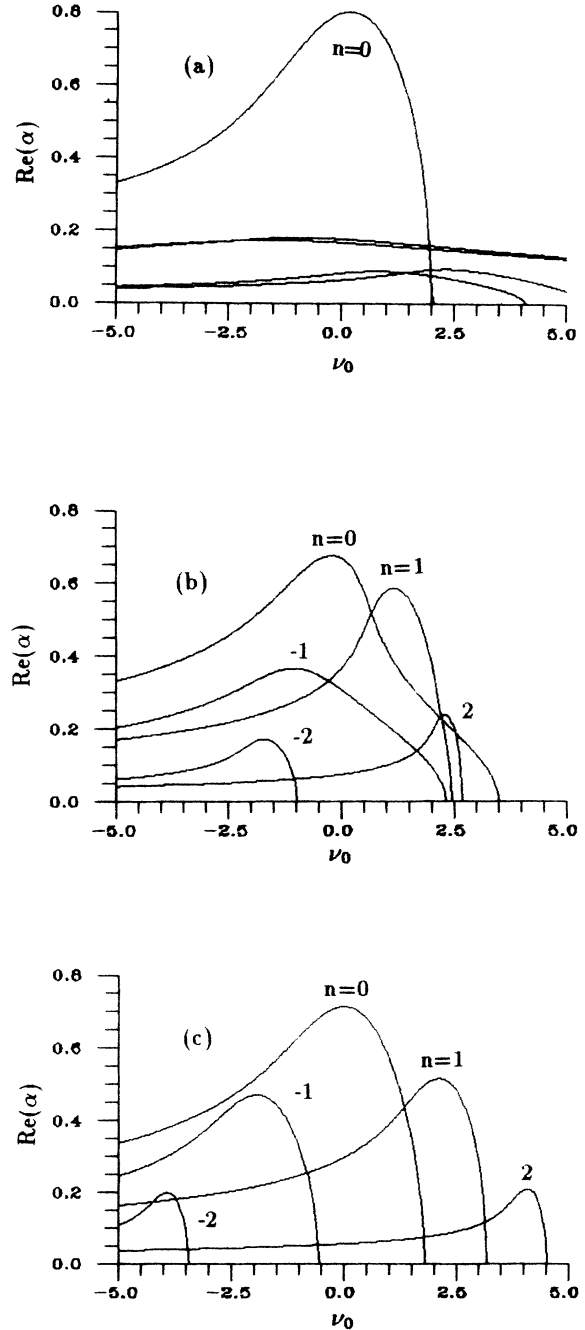


FIG. 1. The growth rate $\text{Re}(\alpha)$ of the many increasing modes is shown as a function of scaled energy detuning ν_0 for (a) $\kappa = 0.4$ and $\sigma = 1$, (b) $\kappa = 1$ and $\sigma = 1$, and (c) $\kappa = 2$ and $\sigma = 1$.

inates the linear dynamics. As σ increases, the maximum growth rate of the first mode may increase to be larger than the growth rate of the zeroth mode, and the linear dynamics is dominated by first mode. The borderline of the zeroth mode dominating domain and the first mode dominating domain is plotted in Fig. 3. It is worth noting that the growth rates of the higher modes ($n=2,3,4,\dots$) may increase to be higher than those of the lower modes ($n=0,1$) as σ is large enough. Then the competition between higher modes may occur for a large σ . Moreover, it is found that the eigenvalue α of the zeroth mode may be equal to that of the first mode under a critical condition. The critical condition is plotted in Fig. 4. We label the left- and right-hand side of the critical condition in the κ and σ planes as the first and the second regimes, respectively. Our analysis shows that the spectral shape of the zeroth mode exists as two peaks when κ and σ are near the critical condition in the first regime. As κ and σ approach to critical condition from the first regime, the peak of the first mode approaches the saddle between the two peaks of the zeroth mode. When κ and σ reach the second regime, the spectral lines of the

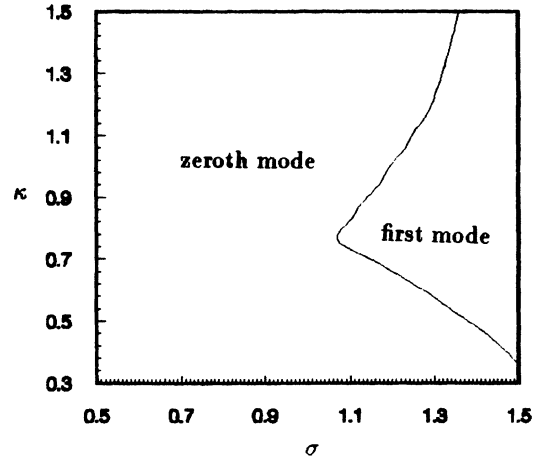


FIG. 3. The borderline of the zeroth mode dominating domain and the first mode dominating domain is shown.

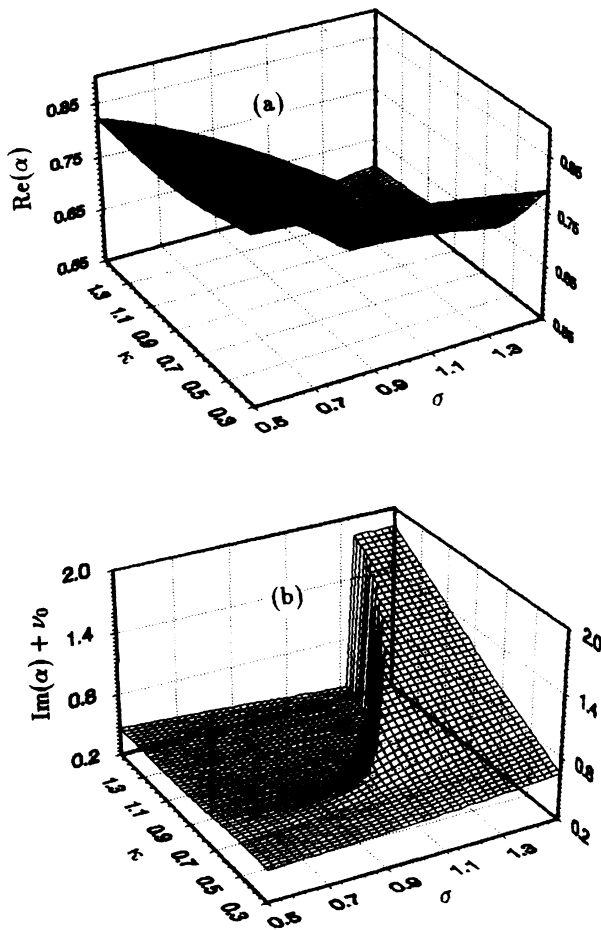


FIG. 2. (a) The maximum growth rate $\text{Re}(\alpha)$ and (b) the phase shift rate $\text{Im}(\alpha + i\nu_0)$ of the most unstable mode is shown as a function of κ and σ , where ν_0 is chosen to maximize the growth rate of the most unstable mode.

two modes on the left-hand side of the cross points are exchanged. This may be better clarified by Fig. 5, in which we compare the growth rate of the zeroth mode and the first mode for (a) $\kappa=0.6$ and $\sigma=1.25$ (solid lines) and $\kappa=0.6$ and $\sigma=1.27$ (dashed lines) and (b) $\kappa=0.9$ and $\sigma=0.83$ (solid lines) and $\kappa=0.9$ and $\sigma=0.85$ (dashed lines). This is the mode transition between the zeroth mode and the first mode in the high-gain TFU FEL. Our numerical results also show that the mode transition between the higher modes may occur as σ is large enough. When $\kappa \leq 0.76$, the zeroth mode's second peak is higher than its first peak as κ and σ are near the critical condition in the first regime [Fig. 5(a)]. In this case, the borderline of the zeroth mode dominating domain and the first mode dominating domain is exactly equal to the critical condition of mode transition between the zeroth mode and the first mode, and then the phase shift rate is continued on both sides of the borderline. When $\kappa > 0.76$, the zeroth mode's first peak is higher than its second peak as κ and σ are near the critical condition in

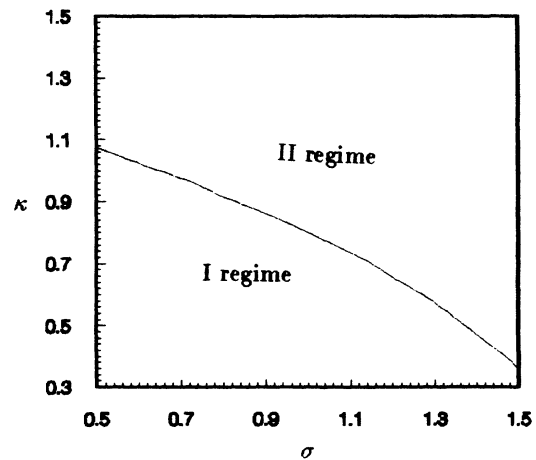


FIG. 4. The critical condition that the eigenvalue α of the zeroth mode is equal to the eigenvalue of the first mode, is plotted.

the first regime [Fig. 5(b)]. In this case, both sides of the critical condition are dominated by the zeroth mode and then the phase shift rate of the most unstable mode is discontinued on the sides of the borderline of the zeroth mode dominating domain and the first mode dominating domain.

Next we will estimate the efficiency of the TFU FEL based on the linear theory. Similar to the nonlinear saturation of the ordinary undulator FEL [15], the nonlinear saturation of TFU FEL may be expected to result from the electron trapped by the ponderomotive potential wells for the most unstable mode. The ponderomotive phase of the n th unstable mode may be written as $\xi_s^{(n)} = (k + k_{w1} + nk_b)\bar{z} - \omega t$. Then the ponderomotive phase velocity of the n th mode may be expressed as

$$v_{ph}^{(n)} = \bar{v}_0 - 2c[\text{Im}(\alpha_n) + \nu_n]/(k + k_{w1})L_G. \quad (3.9)$$

If we assume that the m th mode is the most unstable mode of the high-gain TFU FEL, the efficiency of a TFU FEL may be estimated to be $\eta = (\gamma_0 - \gamma_{ph}^{(m)})/(\gamma_0 - 1)$, where $\gamma_{ph}^{(m)} = [1 - (v_{ph}^{(m)}/c)^2]^{-1/2}$ and γ_0 is the initial

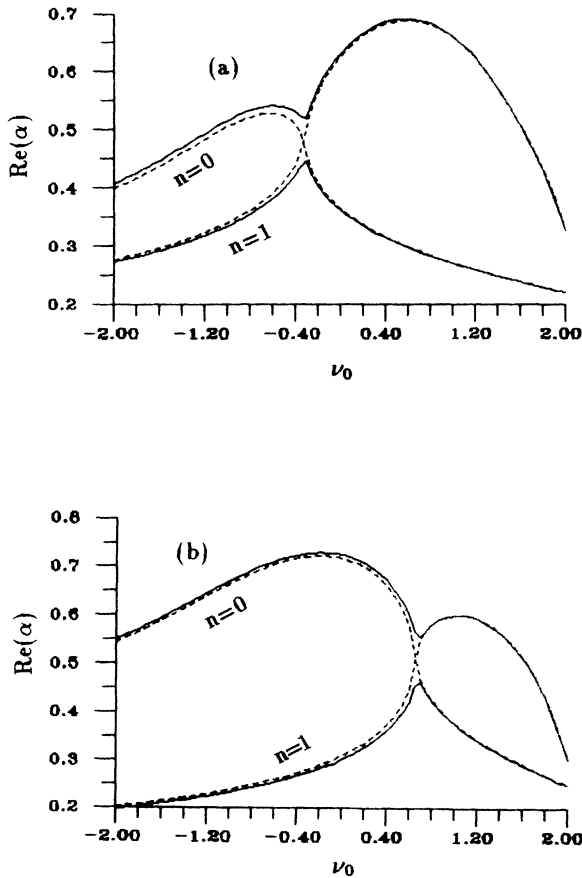


FIG. 5. The growth rate $\text{Re}(\alpha)$ of the zeroth mode ($n=0$) and the first mode ($n=1$) is plotted as a function of energy detuning ν_0 for (a) $\kappa=0.6$ and $\sigma=1.25$ (solid lines) and $\kappa=0.6$ and $\sigma=1.27$ (dash lines) and (b) $\kappa=0.9$ and $\sigma=0.85$ (solid lines) and $\kappa=0.9$ and $\sigma=0.85$ (dash lines).

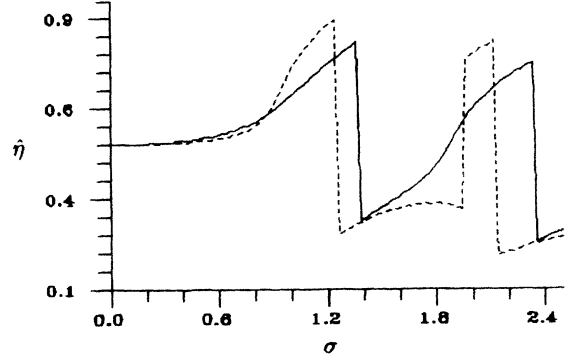


FIG. 6. The efficiency factor $\hat{\eta}$ corresponding to the most unstable mode versus the TFU parameter σ for $\kappa=0.5$ (solid line) and $\kappa=0.6$ (dashed line).

Lorentz factor of the relativistic electron. In the limit of $\gamma_0 \gg 1$, the efficiency may be approximately expressed by

$$\eta \approx \hat{\eta}/k_{w1}L_G, \quad (3.10)$$

with $\hat{\eta} = \text{Im}(\alpha_m) + \nu_m$. Equation (3.10) shows that the efficiency of the TFU FEL is proportional to an efficiency factor $\hat{\eta}$ and inverse to the gain length L_G and the undulator wave number k_{w1} . From the plot of Fig. 2(b), it can be seen that the phase shift rate of the most unstable mode increases with σ in the zeroth mode dominating domain for $\kappa \leq 0.76$. This indicates that, under this condition, the ponderomotive phase velocity of the most unstable mode (zeroth mode) decreases as σ increases, resulting in an efficiency enhancement. In addition, our numerical results show that an efficiency enhancement may be obtained under other conditions. Figure 6 provides an illustration in which the efficiency factor $\hat{\eta}$ is plotted as a function of σ for $\kappa=0.5$ (solid line) and $\kappa=0.6$ (dashed line). The plots in Fig. 6 indicate that the efficiency enhancement also occurs in the first regime when σ approaches the critical condition of the mode transition between the first mode and the second mode. Therefore, one may conjecture that the EBW may reduce the phase velocity of the ponderomotive phase for the most unstable mode and enhance the efficiency of the FEL under proper conditions.

IV. OPTICAL GUIDING IN THE FREE-ELECTRON LASER WITH A TWO-FREQUENCY UNDULATOR

In a one-dimensional analysis of the FEL, the optical field, the undulator, and the relativistic electrons resonantly couple so as to alter the longitudinal wave number of the optical field. This resonant interaction can result in radiation focusing in the FEL [16–18]. In this section, we study optical guiding in the TFU FEL and focus our attention on the effects of the EBW on optical guiding in the weak-field high-gain regime. For simplicity, we treat

the bunching electron beam as if it were an optical fiber with a constant index of refraction and a step edge. The fiber in our analysis consists of a bunched electron beam core of radius r_0 , an index of refraction n_{co} , and a free-space cladding of index $n_{cl}=1$. The index of refraction of an optically bunched electron beam core may be written as [19]

$$n_{co}-1 = \frac{1}{kL_G a_s} \sum_{m,n=-\infty}^{\infty} J_m(\sigma) J_n(\sigma) \int_0^\tau d\tau' \int_0^{\tau'} d\tau'' \exp[-i(\nu_m \tau - \nu_n \tau'')] a_s(\tau''). \quad (4.2)$$

In analogy to the one-dimensional case, assuming that $a_s = a_0 \psi(r) \exp[\int_0^\tau \beta(\tau') d\tau']$, one gets

$$n_{co}-1 = \frac{1}{kL_G} \sum_{n=-\infty}^{\infty} S_n (\alpha + i\nu_n)^{-2}. \quad (4.3)$$

It is known that such an optical fiber always has at least one guided mode, the LP_{01} mode [20], which is expected to be the dominant mode of a FEL [10,11]. Therefore, we restrict our attention to the LP_{01} mode, for which

$$\psi(r) = \begin{cases} J_0(\chi r/r_0) & \text{for } r < r_0 \\ DH_0(\chi_p r/r_0) & \text{for } r > r_0, \end{cases} \quad (4.4)$$

where $D = J_0(\chi)/H_0(\chi_p)$, and H_0 is the Hankel function of the first kind and zeroth order. The complex parameters χ and χ_p are determined by the equations

$$\frac{\chi J'_0(\chi)}{J_0(\chi)} = \frac{\chi_p H'_0(\chi_p)}{H_0(\chi_p)} \equiv R, \quad (4.5)$$

$$\chi^2 - \chi_p^2 \equiv V^2 = (n_{co}^2 - 1) k^2 r_0^2, \quad (4.6)$$

where V is the "normalized frequency parameter" or "V number" of the fiber. Thus α can be expressed in terms of χ_p , which is

$$\alpha = \chi_p^2 L_G / (2ikr_0^2). \quad (4.7)$$

For simplicity, we can make the assumption that the fiber is weakly guiding, i.e., $|n_{co}-1| \ll 1$. This inequality is quite good for all cases of interest and is consistent with the assumption of a slowly varying optical field. Within the confines of this approximation, the V number may be expressed by

$$V^2 = -\hat{C} \sum_{n=-\infty}^{\infty} S_n (\chi_p^2 - \hat{\nu}_n)^{-2}, \quad (4.8)$$

where the dimensionless parameters $\hat{\nu}_n = 2kr_0^2 \nu_n / L_G$ and $\hat{C} = 4k^3 r_0^6 / L_G^3$. The coupled equations (4.5)–(4.8) give a formulation of optical guiding in the linear high-gain regime TFU FEL. In the limit of $\sigma \ll 1$, these equations will reduce to the well-known ordinary equations [16,17]. Equations (4.5)–(4.8) present many resonant points in the phase space and there are many growth modes in the three-dimensional TFU FEL as well as that in the one-dimensional case. The index of the refraction for each

$$n_{co}-1 \equiv \frac{1}{ikL_G a_s} \frac{d}{d\tau} a_s = \frac{i}{kL_G a_s} \langle \exp(-i\xi_s) \rangle, \quad (4.1)$$

where ξ_s is determined by the forcing pendulum equation (2.6) as in the one-dimensional case. Expanding Eqs. (2.6) and (4.1) and keeping to the first order of the optical amplitude a_s , one obtains

unstable mode is generally different from those of the others, which results in a different refractive guide for each mode. This can clearly be understood by inspecting Fig. 7, in which we have plotted the growth rate and the V number of the $n=0, \pm 1, \pm 2$ modes of the three-dimensional results about the parameter \hat{C} for $\kappa=1$ and $\sigma=1$. Obviously, optical guiding effects in the high-gain TFU FEL are greatly dependent upon the dimensionless parameter \hat{C} , like that in the high-gain FEL with an ordinary undulator [16,17]. For small \hat{C} , the growth rate is much smaller than the one-dimensional result, since radiated light would rapidly diffract out of the electron beam before it can get amplified much. For large \hat{C} , the

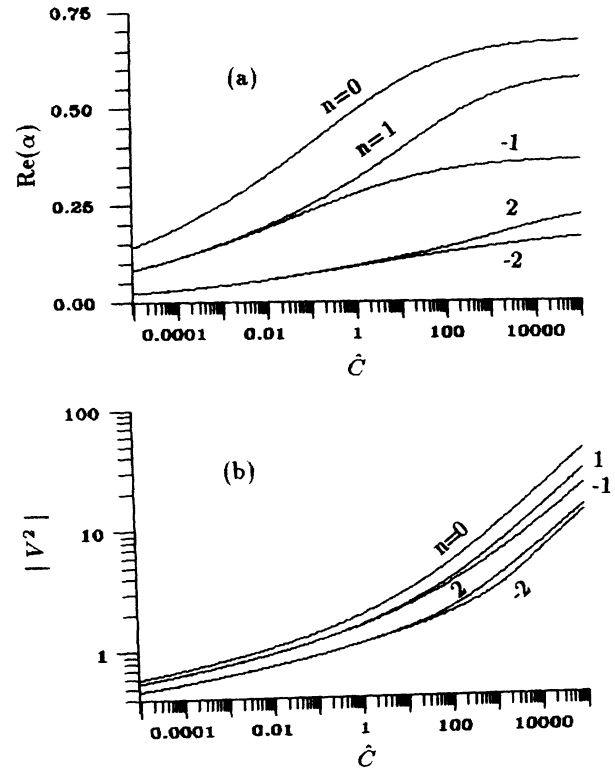


FIG. 7. (a) The V number and (b) maximum growth rate $\text{Re}(\alpha)$ of the many modes, as determined by three-dimensional theory, are shown as a function of the parameter \hat{C} for $\sigma=1$ and $\kappa=1$, where ν_0 is chosen to maximize the growth rate of each mode.

diffractive effects may be relatively unimportant and the optical field is strongly trapped in the beam volume; therefore, growth rate approaches the one-dimensional value.

It is worth expressing the per-pass gain of the high-gain TFU FEL in the form

$$G = G_m \exp[(2L_w/L_G) \operatorname{Re}(\alpha_m)], \quad (4.9)$$

corresponding to the most unstable mode, the m th mode. Here G_m is known as the power coupling coefficient corresponding to the most unstable mode with the growth rate $\operatorname{Re}(\alpha_m)$, which is determined by the initial condition. Following the Green's function methods exploited by Moore [16,17] in the high-gain three-dimensional FEL theory, one may obtain the coefficient G_m , which is given by

$$G_m = |T_m|^2 / |N_m|^2, \quad (4.10)$$

with

$$T_m = \int_0^\infty dr r a_s(0) \psi_m(r), \quad (4.11)$$

$$N_m = \int_0^\infty dr r \psi_m^2(r) \left[1 + 2iu(r) \sum_{l=-\infty}^{\infty} S_l(\alpha_m + i\nu_l)^{-3} \right], \quad (4.12)$$

where $u(r)$ is step edged distribution of the relativistic beam of electrons, i.e., $u(r) = 1$, for $r < r_0$ and $u(r) = 0$ for $r > r_0$. It shows that the coupling coefficient G_m depends on the input optical field as well as the mode of the transverse profile. While the eigenvalue α_m for a given system is fixed, the coupling coefficient G_m varies about the profile of the input optical field. According to previous work [16,17], the maximum value of G_m is reached with $a_s(0) = a_0 \psi_m^*$. In this case, the complex parameters T_m and N_m may be written as

$$T_m = r_0^2 - J_0(\chi_m)^2 (R_m^* - R_m) \times \left[\frac{1}{(\chi_m^2 - \chi_{mp}^{*2})} - \frac{1}{(\chi_{mp}^2 - \chi_m^{*2})} \right], \quad (4.13)$$

$$N_m = \frac{r_0^2}{2} J_1^2(\chi_m) \left[2\hat{C} \sum_{l=-\infty}^{\infty} S_l(\chi_{mp}^2 - \hat{\nu}_l)^{-3} \left[1 + \frac{\chi_m^2}{R_m^2} \right] + 1 - \frac{\chi_m^2}{\chi_{mp}^2} \right]. \quad (4.14)$$

The effects of the EBW on optical guiding in the FEL are better clarified by Fig. 8, in which we compare (a) the maximum growth rate, (b) the V number, and (c) the initial power coupling G_m of the most unstable mode versus \hat{C} for different σ with the effective detuning $\hat{\nu}_0$ being chosen to maximize the growth rate. As Fig. 8(b) illustrates, the V number of the most unstable mode for the FEL is reduced by the EBW, which results in a decrease of the refractive guiding of the radiation. Figure 8(a) shows that the growth rate of the most unstable mode decreases as σ increases. This results from the fact that the EBW cause emission into many unstable modes and

reduces the refractive guiding of the most unstable mode. From Fig. 8(c) it can be seen that the power coupling coefficient of the most unstable mode for the FEL may be enhanced by the EBW under proper conditions. In these plots, the cases of $\sigma = 0, 0.5$, and 1.5 are far from the critical conditions of mode transition, while the cases of

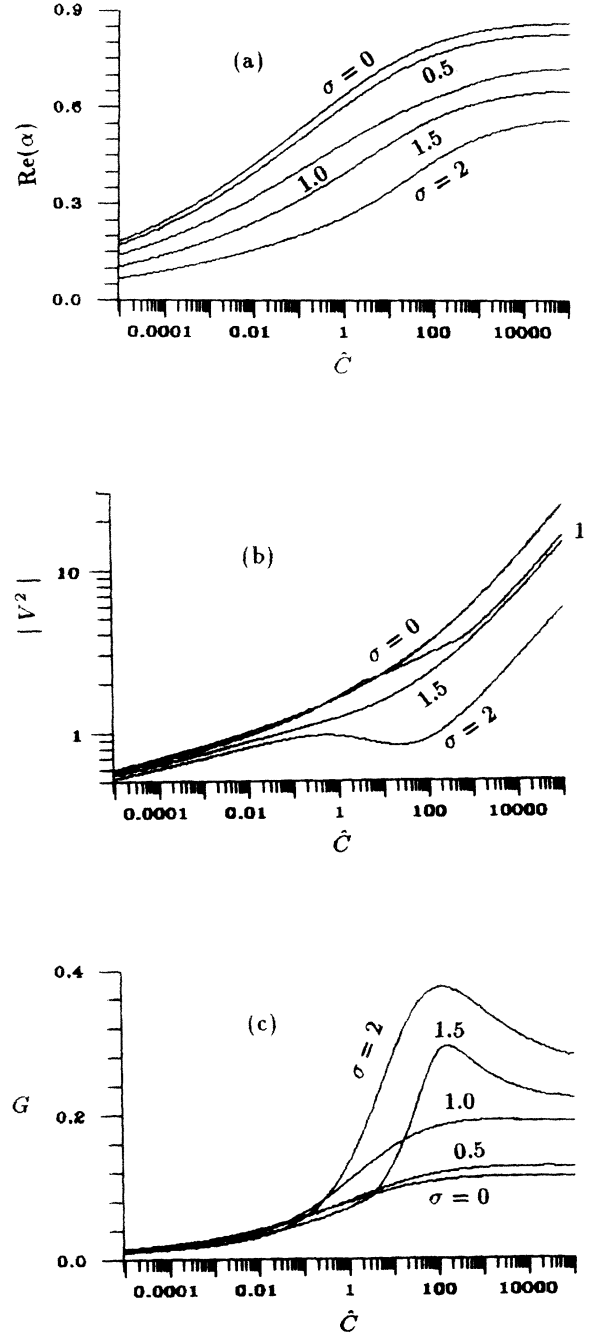


FIG. 8. (a) The V number, (b) maximum growth rate $\operatorname{Re}(\alpha)$, and (c) the power coefficient G of the most unstable growth mode, as determined by three-dimensional theory, are shown as a function of the parameter \hat{C} for different value of σ with $\kappa = 0.6$, where ν_0 is chosen to maximize the growth rate of the most unstable mode.

$\sigma=1$ and 2 approach the critical conditions of mode transition between the zeroth mode and the first mode and of mode transition between the first mode and the second mode, respectively. Therefore, as the TFU parameters κ and σ are far from the critical conditions for the mode transition, the index of the refractive guiding and power coupling coefficients increase with \hat{C} and approach the maximum value for large \hat{C} , which is similar to parameters in the FEL with an ordinary undulator [16,17]. However, when the TFU parameters approach the critical condition of the mode transition, the refractive guiding increases with \hat{C} for small and large \hat{C} , but it decreases with \hat{C} as \hat{C} approaches 10; the power coupling coefficient increases with \hat{C} for small \hat{C} , but it decreases with \hat{C} for large \hat{C} .

It should be noted that we have assumed that the electron transverse oscillation scale is smaller than the radial length structure so that the effect of the relativistic electron beam bending due to the finite radius of the electron wiggling may be neglected. Adding the wiggling motion will decrease gain and increase transverse dimensions [21]. However, these effects are significant only for $K_1 \gg 2\gamma k_{w1} r_0$. Therefore, the smooth boundary approximation in our analysis is valid enough.

V. SUMMARY

In this paper, we have developed a theory of the TFU FEL in the weak-field high-gain regime. A beating wave in the electron's longitudinal motion is excited by the TFU. While the conventional FEL has only one resonant point in phase space, the TFU FEL has many resonant

points in phase space, which are induced by the EBW. Since the EBW may cause emission into many unstable modes, the growth rate of the most unstable mode decreases as σ increases. When the TFU parameter κ is comparable to unity, complex interferences occur between the different resonant points. Due to the complex interferences between the different resonant points, the ponderomotive phase velocity of the most unstable mode may be reduced, resulting in an efficiency enhancement. In this case, the spectrum shapes of the many modes are deeply modified by the complex interferences. Our analysis shows that the zeroth mode dominates the linear dynamics of the TFU FEL for small σ , but the zeroth unstable mode may be overcome by the higher ($n \geq 1$) unstable mode as σ increases.

Furthermore, we have studied the effects of the EBW on optical guiding in the TFU FEL. The three-dimensional high-gain TFU FELs have many unstable modes, as in the one-dimensional case. The refractive guiding of each mode is different from that of the others. Similar to the refractive guiding in the conventional FEL, the refractive guiding in the TFU FEL is greatly dependent upon the parameter \hat{C} . For small \hat{C} , the diffraction loss is important and the gain is much smaller than that of the one-dimensional results. For large \hat{C} , the diffraction loss is negligible and the gain approximately equals the one-dimensional value. Our numerical results show that EBW reduces the refractive guiding and thus increases the diffraction losses. In addition, it is found that the power coupling coefficient of the most unstable mode may be enhanced by the EBW, which may lead to a higher gain.

-
- [1] J. M. J. Madey, *J. Appl. Phys.* **42**, 1906 (1971).
 - [2] S. V. Benson and J. M. J. Madey, *Phys. Rev. A* **39**, 1579 (1989).
 - [3] C. A. Brau, *Free-Electron Lasers* (Academic, New York, 1990).
 - [4] D. Iracane and J. L. Ferrer, *Phys. Rev. Lett.* **66**, 33 (1991).
 - [5] R. W. Warren, J. E. Sollid, D. W. Feldman, W. E. Stein, W. J. Johnson, A. H. Lumpkin, and J. C. Goldstein, *Nucl. Instrum. Methods* **285**, 1 (1989).
 - [6] D. Iracane and P. Bamas, *Phys. Rev. Lett.* **67**, 3086 (1991).
 - [7] D. Iracane and P. Bamas, *Nucl. Instrum. Methods* **318**, 839 (1992).
 - [8] A. T. Lin and J. M. Dawson, *Phys. Rev. Lett.* **42**, 1670 (1979).
 - [9] P. Sprangle, C. M. Tang, and W. M. Mannheimer, *Phys. Rev. Lett.* **43**, 1932 (1979).
 - [10] W. B. Colson, *Phys. Lett.* **64A**, 190 (1977).
 - [11] W. B. Colson, *Phys. Rev. A* **27**, 1399 (1983).
 - [12] W. B. Colson, *Phys. Rev. A* **24**, 639 (1981).
 - [13] W. B. Colson, *IEEE J. Quantum Electron.* **QE-17**, 1417 (1981).
 - [14] R. Bonifacio, L. Narducci, and C. Pellegrini, *Opt. Commun.* **50**, 373 (1984).
 - [15] P. Sprangle and R. A. Simth, *Phys. Rev. A* **21**, 293 (1980).
 - [16] G. T. Moore, *Opt. Commun.* **52**, 46 (1984).
 - [17] G. T. Moore, *Nucl. Instrum. Methods A* **250**, 381 (1986).
 - [18] E. T. Scharlemann, A. M. Sessler, and J. S. Wurtele, *Phys. Rev. Lett.* **54**, 1925 (1985).
 - [19] D. Prosnitz, A. Szoke, and V. K. Neil, *Phys. Rev. Lett.* **24**, 1436 (1981).
 - [20] D. Marcuse, *Theory of Dielectric Waveguides* (Academic, New York, 1974).
 - [21] R. H. Pantell, E. Fontana, and J. Feinstein, *Nucl. Instrum. Methods A* **259**, 143 (1987).

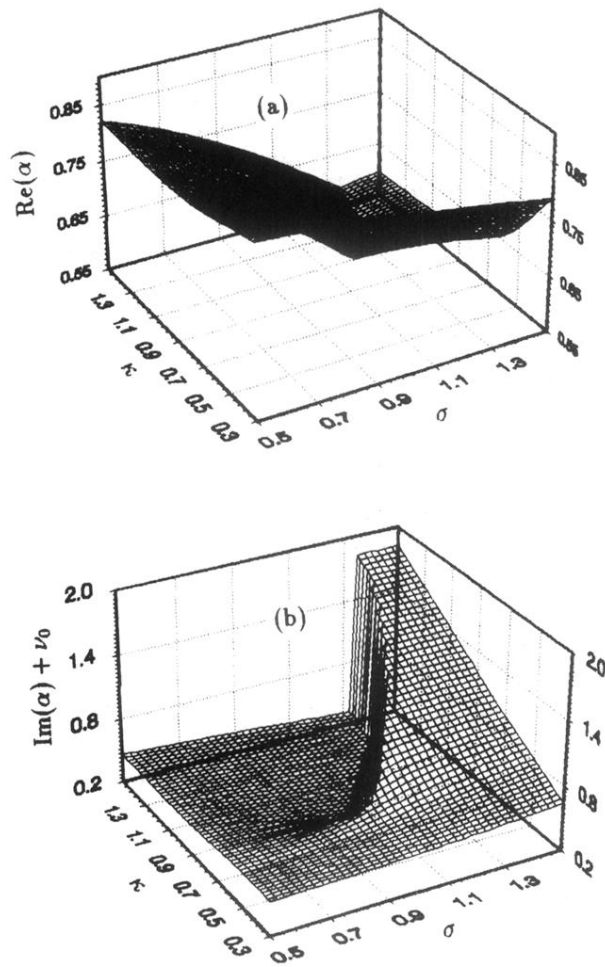


FIG. 2. (a) The maximum growth rate $\text{Re}(\alpha)$ and (b) the phase shift rate $\text{Im}(\alpha + i\nu_0)$ of the most unstable mode is shown as a function of κ and σ , where ν_0 is chosen to maximize the growth rate of the most unstable mode.